An Image-Based Analysis of Torsional Stiffness of Skeletal Elements

Ben Brown, Andrew Rapoff

ABSTRACT Modeling torsional stiffness in the primate skeletal elements is challenging given both variation in cross-sectional geometry and heterogeneity inherent to bone tissue. The computationally simple polar moment of inertia (*J*) is only valid in restricted contexts but is often used out of convenience under the assumption that modest errors ensue. An "exact" solution for torsional stiffness that includes geometrical complexity, loading parameters, boundary conditions, and material variation involves application of structural finite element models whose implementation for comparative purposes is currently impractical.

We have developed a method for approximating the torsional resistance of skeletal elements that incorporates the irregular geometries of and the inhomogeneous bone tissue stiffness distribution within cross sections. Our approximation assumes the corpus to be a prismatic or slightly tapered rod under torsion at each end. We use radiographic grayscale variation to determine an effective shear modulus and thereby arrive at an image-based measure of torsional stiffness.

We apply our method to a sample of great ape mandibular corpus sections. Incorporation of heterogeneity data in addition to geometric information significantly disrupts the rank ordering of individuals within and across samples with regard to relative stiffness. These stiffness values derived under our method are not proportional to corresponding values of *J*; rather, these values are more accurately characterized as being proportional to the reciprocal of *J*. These findings establish that the metrics used to infer torsional stiffness and strength in the literature will, in most cases, fail to predict shear stress and strain values with suitable accuracy.

In the past, measurements of torsional stiffness in skeletal elements take into account element geometry while neglecting significant material properties associated with the element. This sort of technique provides an approximation of the element's torsional stiffness under the assumption that the material is structurally homogeneous in terms of material density. Due to the fact that material density varies at different locations along the bone, certain discrepancies are inherent to this technique. The methods developed in this study provide a procedure for measuring torsional stiffness that includes an assessment of material heterogeneity.

Structural heterogeneity can have a significant effect on the material properties of an element depending on the amount of variation present. The importance of including a measure of structural heterogeneity in torsional stiffness computations can be more easily seen with the help of an analogy presented by Bhatavadekar et al. (2006) in a study examining bending stiffness in skeletal elements. Consider two tubes composed of a relatively malleable material such as rubber; however, one tube is reinforced with steel rods. The reinforced sample will react differently when undergoing forces that produce bending in the element than the simple rubber tube (Bhatavadekar, 2006). The same concept can be applied to elements experiencing torques that produce torsion. The reinforced tube will resist to a greater degree than the simple tube depending on the distribution of steel present in the element, i.e. the degree of heterogeneity.

The present study is closely related to and builds upon the bending stiffness study presented in 2006 by Bhatavadekar et al. This study provides an entirely image-based technique compensating for variation in material density to measure the bending stiffness of the mandibular corpi of three species of great apes. The study uses CT tomography to examine cross-sectional images of a variety of mandible samples. The results show that weighted and unweighted measurement techniques result in error on the order of 10-20% (Bhatavadekar, 2006).

In a similar manner, CT tomography is used in the present study to examine images of cross-sections taken from the premolar regions of mandibles of three species of great apes (*Gorilla, Pongo, and Pan*). CT tomography uses radiographic techniques that allow for imaging of element cross-sections without damaging samples. The CT scan displays a cross-sectional image as a series of pixels. Each pixel incorporates a corresponding grayscale value that makes the image ideal for use in biomechanical studies, such as the present, in which material heterogeneity is a significant factor (Kevles, 1997).

This study applies the torsional stiffness analysis methods to mandibular cross-sections of three species of great apes. The cross-sections are taken from the pre-molar region of the mandible. (To view a diagram of a mandibular corpus, refer to the image in Appendix A. Note, this figure displays a human mandible, whereas the specimens examined in the study are ape mandible). The premolar section was selected as this region was determined to be most reactive to torsion experienced during mastication.

Examination of torsional stiffness in mandibles of great apes can lead to implications in the domain of biological and anthropological behaviors. Biomechanical properties of the mandible may provide significant data relevant to the evolution of dietary habits in different species of great apes. For this reason an accurate measure of torsional stiffness, one that accounts for varying bone density in the mandible, is necessary to the understanding of theories in this realm.

MATERIALS and METHODS

Sample Mandibles and Images

Three CT scans of mandible cross-sections were used in the study. Each image is a mandible scan from 1 of 3 species of great apes: *Gorilla*, *Pongo*, or *Pan*. The images used were attained from studies performed previously (Daegling 1989, 1990; Daegling and Grine, 1991; Bhatavadekar, 2006).

Each image is made up of square pixels that represent 0.49 in. X 0.49 inches in size for the actual mandible itself. The pixel size of the entire image varies from specimen to specimen depending on CT scanning methods utilized in creating the image.

Each of the images used is a cross-sectional image taken from the premolar section of the mandible. For all three images the tooth has been removed through MATLAB code and would fit in the gap at the top of the image as shown in Figure 1. While this at first appears to create a discrepancy when evaluating the torsional stiffness as the mandible no longer appears to take the form of a thin-walled hollow shaft, previous studies have shown that the inclusion of the tooth has little effect on the mechanics of the mandible itself (Bhatavadekar, 2006).

The images were taken using a GE CT 9800 scanner and were converted to grayscale images using applicable software. These tasks were carried out in previous studies (Bhatavadekar, 2006).

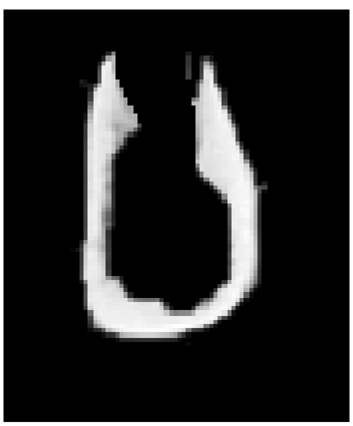

Figure 1 – Converted image of *Pongo* mandible. The image was converted from a CT scan of the specified mandible. The tooth has been removed from the image and would fit in the gap seen at the top of the image.

Weighted Torsional Stiffness

An evaluation of weighted torsional stiffness was made using mechanics theory for the torisonal stiffness (K) of thin-walled shafts. The main equation used are derived from a form of Bredt's formula. This equation involves an examination of a cross-section of the shaft to be studied. Bredt's formula takes the form:

$$K = \frac{4\Gamma^2}{\oint \frac{ds}{G(s)t(s)}}$$

where Γ represents the area of the cross-section enclosed by the midline; s is the natural coordinate around the midline; t is the wall thickness, a function of s; and G is the shear modulus, also a function of s.

In our analysis Bredt's formula is simplified slightly. The line integral is replaced by a summation, since our methods include a segmentation of each image and analysis of each segment individually. Thus, the equation above becomes:

$$K \approx \frac{4\Gamma^2}{\sum \frac{\Delta s}{G(s)t(s)}}$$

Shear modulus (G) is proportional to the density of the material and thus is also proportional to the grayscale of the image being examined. The relationship between density and grayscale takes the form:

$$\rho \propto \lambda^{1/\beta}$$

where ρ and λ represent density and grayscale respectively. Likewise the relationship between shear modulus and density is represented by the equation:

$$G \propto \rho^b$$

Combining the two previous equations results in a relationship between shear modulus and grayscale:

$$G \propto \lambda^{b/\beta} = \lambda^r$$

where λ represents grayscale. In previous studies it has been shown that for all intensive purposes $r \approx 1$ (Bhatavadekar, 2006). Thus a value of 1 was used for r in this study. Taking this into account, the equation becomes:

$$k \approx \frac{4\Gamma^2}{\sum \frac{\Delta s}{\lambda(s)t(s)}}$$

This was the equation used to determine torsional analysis within the study.

Segmentation of Image

Segmentation of the image was carried out using the computer program Adobe Photoshop Elements 3.0. Each segmentation line was superimposed on the CT scan using the line tool incorporated in the program. This tool allows lines to be drawn on the image without affecting the properties of the image itself by creating lines in layers above the actual image, found in the background layer. Thus, the superimposed lines did not interfere with the grayscale values inherent in the image or image segments. Each of the three mandible images for *Pongo* and *Pan* were divided into 37 segments. While the *Gorilla* mandible image was split into 38 segments.

In addition to the segmentation lines, a midline was also superimposed on the mandible image. This line connects the midpoints of each of the segment lines and is important in the analysis of image area. Figure 2 depicts the image of the *Gorilla* mandible with segment lines and midline. The segments of each image are numbered from the first segment to the final segment starting at the left of the figure and following counterclockwise around the mandible.

Once the segmentation lines were drawn, each segment was extracted from the overall image using the Photoshop Elements 3.0 lasso tool. This tool allows the user to create a custom shape, in this case the shape of the segment under investigation. After tracing the edges of each segment and copying the enclosed shape, each segment was thus able to be investigated individually.

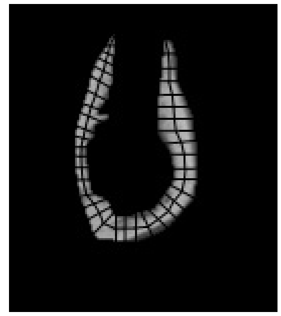

Figure 2 – Image of Gorilla mandible after segmentation lines and midline were superimposed over the image.

Image Analysis – *Δs*

Initial analysis of the segment consisted of determination of the distance along the natural coordinate (s) for each segment in the image. Adobe Photoshop Elements 3.0 allowed us to determine this distance (*Δs*) with the measure tool found in the program. This tool allows the user to click and drag from one point on the image to another, forming a line. The program reports the coordinates of as well as distance between the endpoints. Distance is determined in units of inches on the actual image. Hence, after the *Δs* value for each segment was determined and tabulated, it was necessary to convert from inches on the image to number of pixels. Once this task was performed we were able to determine the value of *Δs* on the actual mandible.

Image Analysis – Thickness (t)

The thickness of each segment is taken as the distance across the mandible perpendicular to the midline. Thickness of each segment was determined in a way similar to the determination of *Δs*. Adobe Photoshop Elements 3.0 was again used and the measure tool was utilized. As seen in Figure 2, thickness varies with position along the s-axis. While most segments have a uniform thickness, the thickness of some segments varies within the segment itself. See Figure 3. For this reason, three values of thickness for each segment were collected using the Photoshop Elements 3.0 measure tool. The mean of these three values produced an average thickness value for the segment.

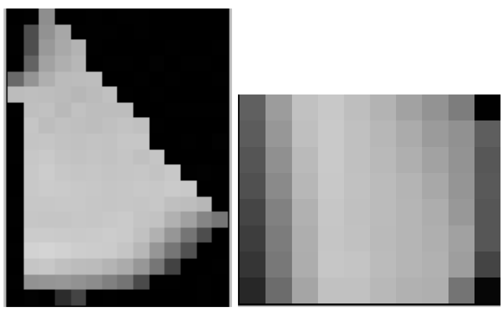

(a) **(b)**

Figure 3 – Each image above represents a segment taken from the image of the *Pan* mandible used in the study. The differences in shape of the segment demonstrate discrepancies in the thickness of each segment: Figure 3a depicts a segment whose thickness varies greatly while Figure 3b shows a segment with nearly uniform thickness. For this reason we used an average thickness for each segment taken from three values determined by measuring the distance across the segment.

Image Analysis – Grayscale Value

Grayscale analysis of individual segments was conducted using the Matlab computer program. This software enabled us to transform the visible image into matrix form. The matrix generated consisted of numbers corresponding to the grayscale value of each pixel in the image. For instance, the first number of the first column of the matrix represents the pixel value of the first pixel in the top left corner of the image; while the final number of the last column of the matrix represents the grayscale value of the pixel located in the bottom right-hand corner of the image.

After converting the segment image into matrix form, the image was written to a Microsoft Excel spreadsheet and the average grayscale value for each segment was then determined and tabulated. Figure 4 depicts a segment extracted from the image of the *Gorilla* mandible and its corresponding matrix.

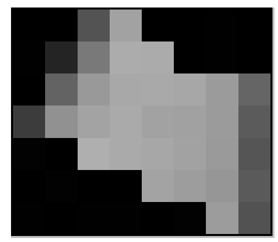

(a)

0	0	84	161	0	0	2	0
1	41	120	170	169	0	2	0
0	99	152	166	167	165	154	101
62	144	162	168	161	159	154	91
3	0	174	168	165	160	153	86
0	3	0	0	162	156	149	90
2	0	1	1	0	3	155	83
				137.9091			

(b)

Figure 4 – The segment depicted in Figure 4a is shown in matrix form in an Excel spreadsheet in Figure 4b. Each value in the matrix corresponds to the pixel value or grayscale value of each pixel in the image. The value at the bottom of the image represents the average, calculated by averaging all values in the matrix and excluding background values. The pixel values corresponding to the black background of the image have a value of 0 or close to 0 (i.e. 1,2).

Image Analysis – Image Area (Γ)

The area enclosed by the midline (Γ) was determined for each of the three sample mandible images. This was completed in a manner similar to the extraction of individual segments from the full image. The Adobe Photoshop Elements 3.0 lasso tool was used to extract the portion of the image enclosed by the midline. The lassoed section was then inserted into a new file and the background filled in with a grayscale differing from the values associated with the area image. The image was converted to a matrix in Matlab and then written to a Microsoft Excel spreadsheet. The number of pixels enclosed by the midline was then determined and tabulated for each of the three sample images. Figure 5 displays an image of the midline area taken from the cross-section of the *Pan* mandible.

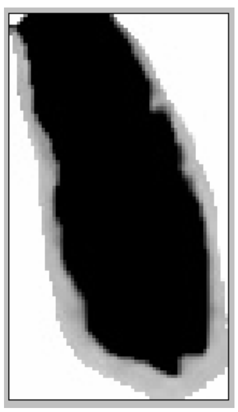

Figure 5 – Image of the area enclosed by the midline taken from the cross-section associated with the *Pan* mandible.

Calculation of Torsional Stiffness

The values of distance along the s-axis (Δs), thickness (t), grayscale (G), and midline area (Γ) were then incorporated into the Bredt's formula for determining torsional stiffness in thin-walled shafts. Three calculations were performed for each of the three sample mandibles: one heterogeneous and two homogeneous. The heterogeneous calculation accounts for inhomogeneous bone density by using individual values of grayscale associated with each segment. The homogenous studies neglect to account for heterogeneity by using identical grayscale values for every segment. In the first homogeneous calculation, the average grayscale of the entire image is used and in the second a grayscale value of 255 (white) is used in the computation.

RESULTS

Comparing Weighted and Unweighted Torsional Stiffness Results

Weighted and unweighted results for torsional stiffness were determined and compared and can be viewed in Figure 5. Results are categorized by great ape genus and values are shown for a weighted distribution as well as each of two homogeneous calculations. The figure shows that the highest value of torsional stiffness is attained for homogeneous solution in which a value of 255 (k_w) was used as a grayscale value throughout the mandible cross-section. Comparison of k and $kavg$ to kw can be seen in Figure 6. It is apparent in this figure that for each species investigated, the value of torsional stiffness calculated using the average grayscale value over the entire cross-section is larger than the stiffness found using material density heterogeneity.

Comparison of Weighted Torisonal Stiffness Across Taxa

Comparing weighted measures across taxa, the data demonstrate that the cross-section taken from the *Pan* mandible displays the highest torsional stiffness, while the lowest value was attained with the *Pongo* mandible used in the study. The highest ratios of k to k_w, and $kavg$ to kw however, are seen in the *Pongo* mandible (Figure 6).

The magnitude of torsional stiffness measurements across taxa differs greatly. The percentage difference across species can be viewed in Table 1 below.

Grayscale Values vs. Cortical Thickness

Grayscale values were also compared at regions of varying thickness along the cross-section. Figure 7 displays a graph of grayscale vs. cortical thickness. As seen in the figure, values of grayscale generally tend to be larger at thicker regions of the bone.

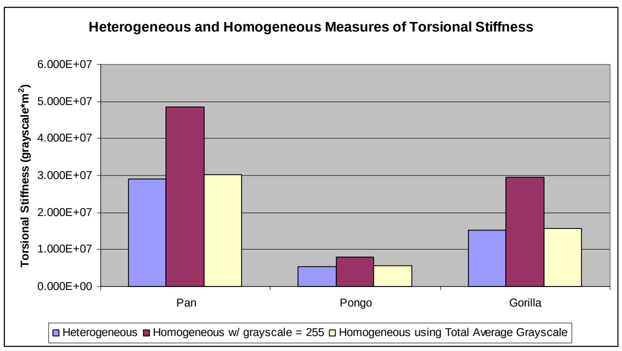

Figure 5 – Figure 5 depicts measures of torsional stiffness. It can be seen that the homogeneous measure using the highest possible grayscale shows the highest torsional stiffness, while the measures of heterogeneous measure is comparable to the homogeneous method that includes a grayscale value equivalent to the total average grayscale taken over the entire mandible cross-section.

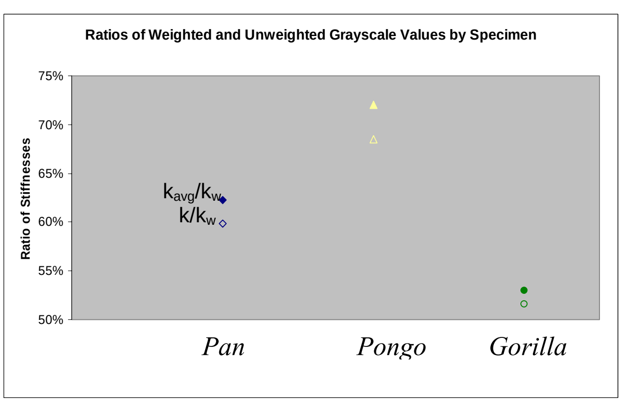

Figure 6 – Figure 6 represents ratios of calculated torsional stiffness values. Each ratio is represented and compared across species.

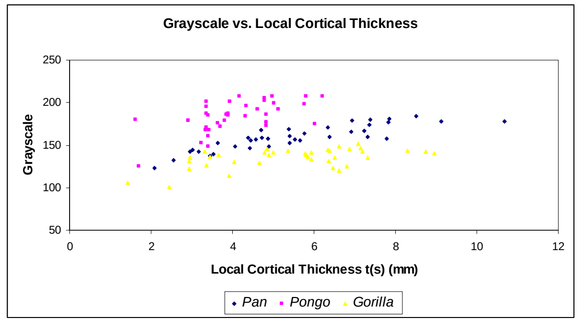

Figure 7 – Figure 7 maps values of segment grayscale values vs. the corresponding value of cortical thickness associated with the same segment.

Pongo vs. *Pan*	81.43%
Pongo vs. *Gorilla*	64.66%
Pan vs. *Gorilla*	47.46%

Table 1 – Table 1 displays differences in heterogeneous grayscale values across taxa. Note that the regardless of taxa, the percentage of difference is high for each comparison.

DISCUSSION

Effects of Grayscale

Measures of torsional stiffness that take into account material heterogeneity are seen to differ by as much as 50-75% over the samples that were investigated. Examination of the ratios of stiffness values (Figure 6) conveys that the stiffness is actually overestimated when average grayscale over the entire cross-section is used as compared with the computation of stiffness using heterogeneous grayscale distribution. These data imply that inclusion of material density variations in torsional stiffness computations is significant. Furthermore, variations in material density with geometry must be taken into consideration in order to attain the most accurate results.

Taxonomic Differences

The high degree of difference in weighted measures of torsional stiffness across the taxa that were studied suggests that mandible samples taken from different taxa have varying degrees of resistance to forces that produce twisting in the elements. As seen in Table 1, differences of approximately 50-80% were noted across taxa for the regions of the mandible under investigation. Discrepancies of this magnitude may have significance in terms of evolutionary mandible mechanics across taxa. Furthermore, the inconsistencies observed may have particular relevance in terms of differences in dietary habits across great ape taxa. In order to justify this sort of inference, however, a great deal more research into the anthropological habits of great apes is necessary.

While this study provides a method for determining a weighted measure of torsional stiffness in mandibles of great apes, it is important to realize that assumptions concerning evolutionary or anthropological habits of the taxa under investigation have yet to be proven substantial. This study is more concerned with the development of a process through which accurate measures of torsional stiffness can be determined for the mandible corpus. Justification of the implications of the process and any conclusions drawn from the process can be accomplished by extension of the study to include a greater amount and variety of samples. Additional locations along the bone, i.e. molar and sympheseal sections, should be considered as well in an attempt to arrive at the most accurate conclusions.

Examination of Cortical Thickness

Contrary to prior hypotheses, the grayscale and stiffness values appear to increase at regions of the bone where the cortical thickness is larger. It had been previously theorized that evolutionary trends resulted in stiffer material at thinner sections of the bone. In this way material density would compensate for variations in bone geometry. However, as seen in Figure 6, values of grayscale are higher at areas of greater cortical thickness, in effect contradicting this hypothesis.

CONCLUSIONS

The current study presents a method for determining a weighted measure of torsional stiffness in the premolar region of mandibles of three species of great apes. The process involves an analysis based on mechanical principles involving torsion in thin-walled hollow elements and a variation of Bredt's formula. By using CT images of the mandibles taken at the premolar region, we were able to include an analysis of the geometrically varying material density in our computations. The procedure and methods presented can be readily applied to a larger set of comparative samples from a greater variety of primate sections.

Additionally, the study shows the importance of geometrically varying material density. Likewise, the study has important implications as to material density at areas of increased bone thickness. The study appears to contradict the prior hypothesis that bone density is greater at regions of higher corical thickness.

ACKNOWLEDGEMENTS

Aaron Agostino aided in understanding of tools and functions associated with Adobe Photoshop Elements 3.0.

David Daegling of the University of Florida collaborated in the study.

LITERATURE CITED

Bhatavadekar, Neel B., Daegling, David J., and Rapoff, Andrew J. 2006. Application of an Image-Based Weighted Measure of Skeletal Bending Stiffness to Great Ape Mandibles. Am J of Phsycial Anthroplogy.

Daegling, DJ. 1989. Biomechanics of cross-sectional size and shape in the hominoid mandibular corpus. Am J of Physical Anthropology 80:91-106.

Daegling, DJ. 1990. Geometry and biomechanics of hominoid mandibles, Ph.D dissertation, State University of New York, Stony Brook.

Daegling, DJ and Grine FE. 1991. Compact bone distribution and biomechanics of early hominid mandibles. Am J of Physical Anthropology 86:321-339.

Kevles, Bettyann Holtzman. Naked to the Bone. pp. 145-172. 1997 New Jersey.

APPENDIX A

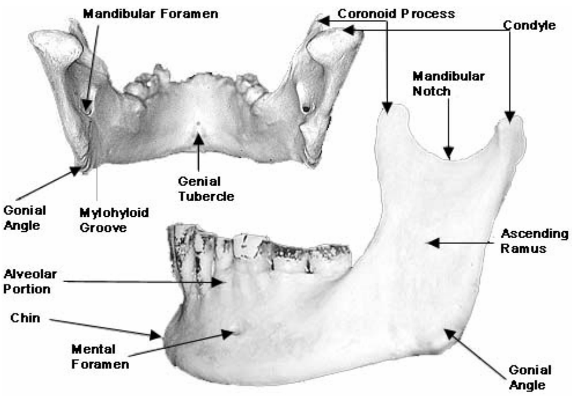

Figure A – This is an image showing key parts of the mandible. Note that this image diagrams a human mandible, while the mandibles analyzed are taken from great apes.
http://medlib.med.utah.edu/kw/osteo/osteology/bonemand.html

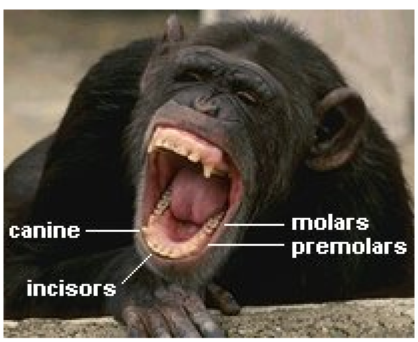

Figure B – The image above shows the premolar region of the mandible and its location relative to other regions of the mandible.
http://images.google.com/imgres?imgurl=http://anthro.palomar.edu/animal/images/mammalian_dentition.jpg&imgrefurl=http://anthro.palomar.edu/animal/animal_4.htm&h=164&w=205&sz=11&tbnid=cF7hQU9x7dMwvM:&tbnh=80&tbnw=100&hl=en&start=13&prev=/images%3Fq%3Dpremolar%26svnum%3D10%26hl%3Den%26lr%3D%26sa%3DN

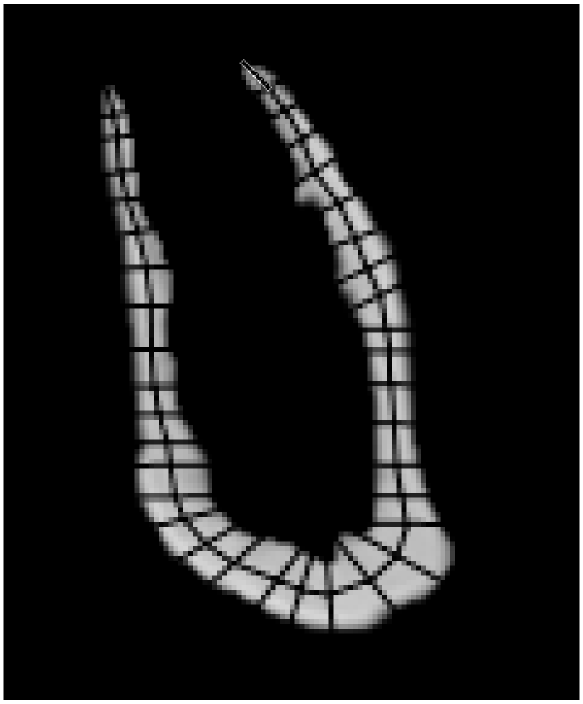

Figure C – Chimpanzee (*Pan*) image after being segmented and with midline drawn.

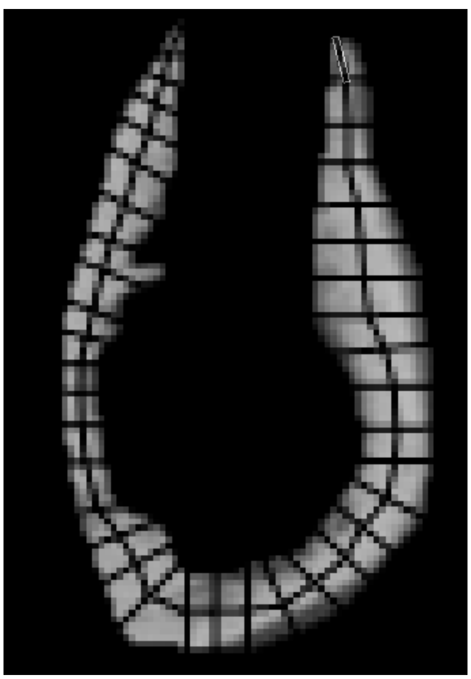

Figure D – Gorilla (*Gorilla*) image after segmentation and with midline drawn

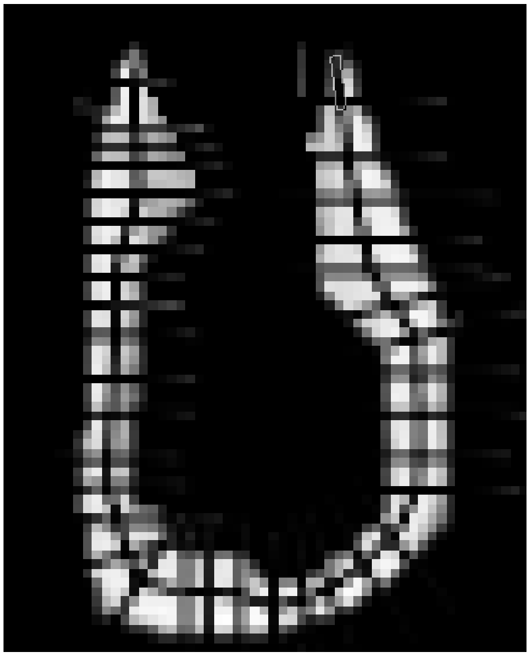

Figure E – Orangutan (*Pongo*) image with segments and midline drawn